Extended-Hückel Energy Band Structures of Transition Metal Compounds with One-Dimensional Crystal Geometries

Basic Equations and Computational Results for Bis(2,5-dimethyl-N,N′-dicyanoquinonediimine) copper(I)

Wolfhard Koch and Friedrich Franz Seelig
Institut für Physikalische und Theoretische Chemie der Universität Tübingen

Z. Naturforsch. **42 a**, 875–888 (1987); received April 10, 1987

Using symmetry adapted basis sets of linearly combined Bloch sums, we summarize the basic equations for one-dimensional energy band structure calculations of extended-Hückel type such as SCC (Self-Consistence of Charge) and SCCC (Self-Consistence of Charge and Configuration). In addition to the considerable computational savings achievable by this technique, its main advantage is that band indexing difficulties can be systematically excluded. Furthermore, it turns out that backtransformations into the original atomic orbital basis are unnecessary throughout. As an illustrative example, we document the energy band structure of a one-dimensional model geometry of highly conducting bis(2,5-dimethyl-N,N′-dicyanoquinonediimine)copper(I) (2,5-DM-DCNQI)$_2$Cu. In spite of its one-electron nature, the outlined energy band structure calculation method appears to be useful to rationalize the unusual electronic properties of this "organic metal".

1. Introduction

In this paper we report the formalism to calculate the *extended-Hückel energy band structure* of transition metal compounds with purely one-dimensional model geometries of isolated stacks with translational symmetry in only one direction and additional spatial symmetries properly characterized by *line groups*. Such *one-dimensional crystals* are taken to be chemically homogeneous and to have no defects. They are assumed to consist of a finite but huge number of one-dimensional unit cells; different geometries and compositions of the terminating cells will be ignored.

Although the extended-Hückel procedure is methodically simple, a considerable amount of computer time and storage capacity is required for band-structure calculations of one-dimensional crystals with many basis orbitals per unit cell. Ab-initio methods based on the Hartree-Fock approximation cannot be applied in these cases. Some sophistication, however, has been brought into the semiempirical self-consistent field (SCF) treatment by Böhm who parametrized such approaches for transition metal compounds [1].

Recently, the synthesis of the highly conducting compound bis(2,5-dimethyl-N,N′-dicyanoquinonediimine)copper(I) (2,5-DM-DCNQI)$_2$Cu has been reported by Aumüller, Erk, Klebe, Hünig, Schütz, and Werner [2] together with the main features of its anisotropic crystalline structure. A one-dimensional model of this interesting "organic metal" will serve us as an example to illustrate the computational method which will be outlined in the following section.

Reprint requests to Dr. W. Koch, Institut für Physikalische und Theoretische Chemie der Universität Tübingen, Auf der Morgenstelle 8, D-7400 Tübingen 1, Federal Republic of Germany.

2. Extended-Hückel Band Structure Calculations of One-Dimensional Crystals

The standard eigenvalue problem of one-dimensional one-electron band theory in a basis set of *M Bloch sums*

$$\{|\Phi_\mu(k)\rangle \,|\, \mu = 1, 2, \ldots, M\} \tag{1}$$

for each *wavenumber* k in the *first Brillouin zone* $-\frac{\pi}{a} < k \leqq \frac{\pi}{a}$ reads:

$$\mathbf{H}(k)\,\mathbf{C}(k) = \mathbf{S}(k)\,\mathbf{C}(k)\,\mathbf{E}(k)\,. \tag{2}$$

0932-0784 / 87 / 0800-0875 $ 01.30/0. – Please order a reprint rather than making your own copy.

$\mathbf{C}(k)$ is the coefficient matrix of the *crystal orbital* expansion

$$|\Psi_i(k)\rangle = \sum_{\mu=1}^{M} C_{\mu i}(k)\,|\Phi_\mu(k)\rangle, \quad i = 1, 2, \ldots, M, \tag{3}$$

$\mathbf{E}(k)$ is the diagonal matrix of the corresponding crystal orbital energies $E_i(k)$, and $\mathbf{S}(k)$ is the overlap matrix of the non-orthogonal basis (1) with elements of the form

$$(\mathbf{S}(k))_{\mu\nu} = S_{\mu\nu}(k) = \langle \Phi_\mu(k)\,|\,\Phi_\nu(k)\rangle \approx \sum_{t=-N_{\max}}^{N_{\max}} \exp(ikta)\,\langle \Phi_\mu^0\,|\,\Phi_\nu^t\rangle, \tag{4}$$

constructed from *M atomic orbitals*

$$\{|\Phi_\mu^0\rangle\,|\,\mu = 1, 2, \ldots, M\} \tag{5}$$

located in the zeroth unit cell of the considered one-dimensional crystal. $N_{\max}$ is that unit-cell index t where the absolute values of *all* integrals $\langle \Phi_\mu^0\,|\,\Phi_\nu^{N_{\max}}\rangle$ remain below a chosen parameter δ for the first time:

$$|\langle \Phi_\mu^0\,|\,\Phi_\nu^{N_{\max}}\rangle| < \delta \quad \text{for all } \mu, \nu. \tag{6}$$

Overlap integrals between atomic orbitals of centers that are $t > N_{\max}$ unit cells apart are completely neglected. In one-electron theory the Hamiltonian $\mathscr{H}$ for a one-dimensional crystal with N unit cells and K electrons per unit cell is supposed to be a sum of $N \cdot K$ effective one-electron operators

$$\mathscr{H} = \sum_{i=1}^{N\cdot K} h_{\text{eff}}(i), \tag{7}$$

where h_{eff} is completely specified by the elements of its matrix representation $\mathbf{H}(k)$ in the set of M Bloch sums (1):

$$(\mathbf{H}(k))_{\mu\nu} = H_{\mu\nu}(k) = \langle \Phi_\mu(k)\,|\,h_{\text{eff}}\,|\,\Phi_\nu(k)\rangle. \tag{8}$$

2.1 *Introduction of a Symmetry-Adapted Basis*

If the idealized one-dimensional crystal possesses in addition to the translational symmetry other symmetry elements such as an n-fold rotation axis C_n identical with the *invariant line* or an equally oriented mirror plane σ_v, computational savings can be achieved and band-indexing difficulties can be avoided by introducing *symmetry-adapted linear combinations* of Bloch sums

$$\{|\Phi_\mu(k, \Gamma_m)\rangle\,|\,\mu = 1, 2, \ldots, \dim V_{k,\Gamma_m}\} \tag{9}$$

as basis functions for each *irreducible representation* Γ_m of a line group $\mathbf{L}$ which characterizes the symmetry properties of the one-dimensional crystal under consideration. The original function space V_k with dimension $\dim V_k = M$ spanned by the basis set of M Bloch sums (1) can be divided in those cases into at least two subspaces V_{k,Γ_m} with lower dimensions $\dim V_{k,\Gamma_m}$:

$$\dim V_k = \sum_{\Gamma_m} \dim V_{k,\Gamma_m} = M. \tag{10}$$

This basis transformation is accomplished by rectangular $(M \times \dim V_{k,\Gamma_m})$-dimensional matrices $\mathbf{\Theta}(k, \Gamma_m)$ which decompose the original $(M \times M)$-dimensional eigenvalue problem (2) into at least two $(\dim V_{k,\Gamma_m} \times \dim V_{k,\Gamma_m})$-dimensional equations

$$\mathbf{H}(k, \Gamma_m)\,\mathbf{C}(k, \Gamma_m) = \mathbf{S}(k, \Gamma_m)\,\mathbf{C}(k, \Gamma_m)\,\mathbf{E}(k, \Gamma_m) \tag{11}$$

with

$$\mathbf{H}(k, \Gamma_m) = \mathbf{\Theta}^\dagger(k, \Gamma_m)\,\mathbf{H}(k)\,\mathbf{\Theta}(k, \Gamma_m) \tag{12}$$

and

$$\mathbf{S}(k, \Gamma_m) = \mathbf{\Theta}^\dagger(k, \Gamma_m)\,\mathbf{S}(k)\,\mathbf{\Theta}(k, \Gamma_m). \tag{13}$$

Each equation (11) can be solved separately to get the coefficient matrices $\mathbf{C}(k, \Gamma_m)$ and the diagonal matrices $\mathbf{E}(k, \Gamma_m)$ of eigenvalues of the corresponding crystal orbital expansions

$$|\Psi_i(k, \Gamma_m)\rangle = \sum_{\mu=1}^{\dim V_{k,\Gamma_m}} C_{\mu i}(k, \Gamma_m)\,|\Phi_\mu(k, \Gamma_m)\rangle, \quad i = 1, 2, \ldots, \dim V_{k,\Gamma_m} \tag{14}$$

in the *symmetry orbitals basis* (9).

How such symmetry orbitals can be constructed and how the elements of the transformation matrices $\mathbf{\Theta}(k, \Gamma_m)$ can be gained, has been described elsewhere for any line group $\mathbf{L}$ isogonal to a point group $\mathbf{C}_n$ or $\mathbf{C}_{nv}$ [3].

2.2 *Overlap Matrices*

In extended-Hückel band theory, overlap integrals (4) between the M non-orthogonal Bloch sums (1) constructed from M s, p, and d *valence shell atomic orbitals* (5) per unit cell have to be calculated explicitly.

The valence shell atomic orbitals characterized by the quantum numbers n, l and m are functions of the spherical polar coordinates r, ϑ and φ:

$$\Phi_{n,l,m}(r, \vartheta, \varphi) = R_{n,l}(r)\,Y_{l,m}(\vartheta, \varphi). \tag{15}$$

$Y_{l,m}(\vartheta, \varphi)$ are the spherical harmonics, and the radial parts $R_{n,l}(r)$ are of Slater type:

$$R_{n,l}(r) = \frac{(2\zeta)^{n+\frac{1}{2}}}{((2n)!)^{\frac{1}{2}}} \cdot r^{n-1} \exp(-\zeta r). \tag{16}$$

Several parameter sets have been recommended for a choice of the *orbital exponents* ζ [4]. Moreover, the radial parts of atomic d orbitals are often chosen to be composed of two radial functions with different orbital exponents ζ_1 and ζ_2 [5]:

$$R_{n,d}(r) = c_1 R_{n,d,\zeta_1}(r) + c_2 R_{n,d,\zeta_2}(r). \tag{17}$$

The computation of overlap integrals $\langle \Phi_\mu^0 | \Phi_\nu^t \rangle$ usually is a time-consuming part of any extended-Hückel calculation; they can be evaluated according to Silver and Ruedenberg [6], for instance.

Because of their Hermitian property

$$\mathbf{S}(k) = \mathbf{S}^\dagger(k) \tag{18}$$

only triangular overlap matrices actually have to be computed. Subsequently, the transformation (13) has to be performed to get the $\mathbf{S}(k, \Gamma_m)$.

2.3 Extended-Hückel Matrices

Several formulas have been proposed for the semiempirical modelling of extended-Hückel matrices [7]. For the Wolfsberg-Helmholz formula (cf. [7]), extended-Hückel matrix elements $H_{\mu\nu}(k, \Gamma_m)$ can be evaluated directly from the $S_{\mu\nu}(k, \Gamma_m)$ according to the following expressions [8, 9]:

$$H_{\mu\nu}(k, \Gamma_m) = -\tfrac{1}{2} F S_{\mu\nu}(k, \Gamma_m)(V_\mu + V_\nu) \quad \text{for} \quad \mu \neq \nu, \tag{19}$$

$$H_{\mu\mu}(k, \Gamma_m) = -V_\mu [1 + F(S_{\mu\mu}(k, \Gamma_m) - 1)]. \tag{20}$$

Therefore the transformation (12) actually needs not to be performed. Appropriate *valence orbital ionization potentials* V_μ (VOIP) of an electron in the μth valence orbital (5) of a neutral atom are available from the tables of reference [10].

If the adjustable parameter F is replaced by another scaling factor F'

$$F' = F + \Delta^2 + \Delta^4(1 - F) \tag{21}$$

with

$$\Delta = \frac{V_\mu - V_\nu}{V_\mu + V_\nu}, \tag{22}$$

the expressions (19) and (20) are also valid for the modified Wolfsberg-Helmholz formula proposed by Ammeter et al. [7]. Like the overlap matrices $\mathbf{S}(k, \Gamma_m)$, extended-Hückel matrices $\mathbf{H}(k, \Gamma_m)$ are also Hermitian:

$$\mathbf{H}(k, \Gamma_m) = \mathbf{H}^\dagger(k, \Gamma_m). \tag{23}$$

2.4 Symmetrical Löwdin Orthogonalization

The symmetrical orthogonalization procedure which transforms the non-orthogonal symmetry orbitals (9) into an orthogonal basis set

$$\{ | \Phi'_\mu(k, \Gamma_m) \rangle \mid \mu = 1, 2, \ldots, \dim V_{k,\Gamma_m} \} \tag{24}$$

by means of the transformation matrix $\mathbf{S}^{-\frac{1}{2}}(k, \Gamma_m)$ consists of two steps [11]:

1. Since $\mathbf{S}(k, \Gamma_m)$ is Hermitian, it can be diagonalized [12] by a unitary matrix $\mathbf{U}(k, \Gamma_m)$:

$$\mathbf{U}^\dagger(k, \Gamma_m)\, \mathbf{S}(k, \Gamma_m)\, \mathbf{U}(k, \Gamma_m) = \mathbf{s}(k, \Gamma_m), \tag{25}$$

where $\mathbf{s}(k, \Gamma_m)$ is a diagonal matrix of the eigenvalues of $\mathbf{S}(k, \Gamma_m)$. The Hermitian transformation matrix $\mathbf{S}^{-\frac{1}{2}}(k, \Gamma_m)$ is constructed by taking the inverse square root of each of the eigenvalues [14] to form the diagonal matrix $\mathbf{s}^{-\frac{1}{2}}(k, \Gamma_m)$ and then "undiagonalizing" by the transformation

$$\mathbf{U}(k, \Gamma_m)\, \mathbf{s}^{-\frac{1}{2}}(k, \Gamma_m)\, \mathbf{U}^\dagger(k, \Gamma_m) \equiv \mathbf{S}^{-\frac{1}{2}}(k, \Gamma_m). \tag{26}$$

2. Substitution of the relation

$$\mathbf{C}(k, \Gamma_m) = \mathbf{S}^{-\frac{1}{2}}(k, \Gamma_m)\, \mathbf{C}'(k, \Gamma_m) \tag{27}$$

between the coefficient matrices $\mathbf{C}(k, \Gamma_m)$ and $\mathbf{C}'(k, \Gamma_m)$ of the non-orthogonal basis (9) and the orthogonal basis (24), respectively, into the eigenvalue equation (11) and multiplication on the left by

$$(\mathbf{S}^{-\frac{1}{2}}(k, \Gamma_m))^\dagger = \mathbf{S}^{-\frac{1}{2}}(k, \Gamma_m) \tag{28}$$

yields

$$\underbrace{\mathbf{S}^{-\frac{1}{2}}(k, \Gamma_m)\, \mathbf{H}(k, \Gamma_m)\, \mathbf{S}^{-\frac{1}{2}}(k, \Gamma_m)}_{\mathbf{H}'(k, \Gamma_m)}\, \mathbf{C}'(k, \Gamma_m)$$

$$= \underbrace{\mathbf{S}^{-\frac{1}{2}}(k, \Gamma_m)\, \mathbf{S}(k, \Gamma_m)\, \mathbf{S}^{-\frac{1}{2}}(k, \Gamma_m)}_{\mathbf{1}}\, \mathbf{C}'(k, \Gamma_m)\, \mathbf{E}(k, \Gamma_m). \tag{29}$$

With the definition of new extended-Hückel matrices

$$\mathbf{H}'(k, \Gamma_m) = \mathbf{S}^{-\frac{1}{2}}(k, \Gamma_m)\, \mathbf{H}(k, \Gamma_m)\, \mathbf{S}^{-\frac{1}{2}}(k, \Gamma_m) \tag{30}$$

in the orthogonalized symmetry orbital basis (24), the final eigenvalue problem reads

$$\mathbf{H}'(k, \Gamma_m)\,\mathbf{C}'(k, \Gamma_m) = \mathbf{C}'(k, \Gamma_m)\,\mathbf{E}(k, \Gamma_m)\,. \qquad (31)$$

2.5 *Eigenvectors and Eigenvalues*

Solving the eigenvalue equation (31) for each wavenumber k and each irreducible representation Γ_m means finding a unitary coefficient matrix $\mathbf{C}'(k, \Gamma_m)$ which transforms the Hermitian matrix $\mathbf{H}'(k, \Gamma_m)$ into the diagonal matrix $\mathbf{E}(k, \Gamma_m)$ of its eigenvalues:

$$(\mathbf{C}'(k, \Gamma_m))^{\dagger}\,\mathbf{H}'(k, \Gamma_m)\,\mathbf{C}'(k, \Gamma_m) = \mathbf{E}(k, \Gamma_m)\,. \qquad (32)$$

This standard problem of numerical quantum chemistry can be solved efficiently by means of the already mentioned diagonalization algorithms [12].

Backtransformation of the eigenvector matrix $\mathbf{C}'(k, \Gamma_m)$ according to (27) leads to the corresponding matrix $\mathbf{C}(k, \Gamma_m)$ in the original non-orthogonal symmetry orbital basis (9).

The energy band structure of occupied valence bands and unoccupied conduction bands is recognizable whenever a band index can be assigned to the eigenvalues of each wavenumber k and each irreducible representation Γ_m. To decide whether a one-dimensional crystal will be electronically conducting, semiconducting or insulating, the electronic crystal orbital occupancy is crucial. Band indexing and band occupation determine the prediction of qualitative electronic and magnetic properties of the one-dimensional system under consideration.

2.5.1 *Indexing of Energy Bands*

The μth energy band of an irreducible representation Γ_m is formed from the ensemble of all crystal orbitals $\Phi_\mu(k, \Gamma_m)$ of the first Brillouin zone $-\frac{\pi}{a} < k \leqq \frac{\pi}{a}$.

In practice, however, only crystal orbitals of those N_k wavenumbers k will be known, for which the corresponding eigenvalue equation (11) has been solved. The assignment Γ_m to each orbital $\Phi_\mu(k, \Gamma_m)$ prevents that crystal orbitals of different irreducible representations are collected within the same energy band.

Assuming cyclic translational symmetry for a considered one-dimensional crystal, it is sufficient to solve (11) only for wavenumbers k within the range $0 \leqq k \leqq \frac{\pi}{a}$, because crystal orbital energies are symmetric with respect to the center of the first Brillouin zone [15]:

$$\mathrm{E}_\mu(k, \Gamma_m) = \mathrm{E}_\mu(-k, \Gamma_m)\,. \qquad (33)$$

The assignment of a band index μ to a crystal orbital, characterized by a wavenumber k and an irreducible representation Γ_m, has to be performed in energetically ascending order. The energy range between the lowest and the highest eigenvalue with band index μ and symmetry label Γ_m is the μth allowed zone of the irreducible representation Γ_m.

The essential advantages of this band indexing procedure using the symmetry label Γ_m are:

- Band indexing difficulties [16] do not occur [17].
- Linearly interpolated, continuous curves $E_{\Gamma_m,\mu}(k)$ with equal Γ_m and different μ do not intersect each other.
- Misinterpretations of the qualitative characteristic of electronic conductivity caused by a wrong band-index assignment can be excluded.

2.5.2 *Occupation of Energy Bands*

Electronic and magnetic properties of one-dimensional crystals are essentially determined by the kind and degree of occupation of the highest occupied energy band. If N_k is the number of k's, for which the eigenvalue equation (11) had been solved, then $N_k \cdot K$ electrons have to be distributed in the total number of $N_k \cdot M$ crystal orbitals.

A non-magnetic insulating state is characterized by completely filled valence bands and a broad energy gap between the highest occupied (HOCO) and the lowest unoccupied crystal orbital (LUCO). A small energy gap leads to a semiconducting state. Metallic conductivity occurs only if the energy gap vanishes.

One-dimensional crystals with an odd number of electrons per unit cell have at least one partially occupied valence band. If the unit cell contains an even number of electrons, partially filled valence bands occur only in the case of an overlap of

different energy bands near the *Fermi level*. In one-electron band theory, a metallic state which arises whenever only the lowest orbitals of an incomplete filled energy band are occupied, is always predicted to be most stable because the total electronic energy $\mathscr{E}$ of the ground state is equal to the sum of its orbital energies multiplied by their corresponding occupation numbers $n_\mu(k, \Gamma_m) \in \{0, 1, 2\}$:

$$\mathscr{E} = \sum_k \sum_{\Gamma_m} \sum_\mu n_\mu(k, \Gamma_m)\, \mathrm{E}_\mu(k, \Gamma_m)\,. \tag{34}$$

Additional reductions of the total electronic ground state energy $\mathscr{E}$ may be caused by geometric *Peierls distortions* of the one-dimensional lattice, by means of which a metallic characteristic may change into a non-magnetic insulating one. But even if Peierls distortions can be excluded, several insulating states [19] are imaginable, whose total electronic ground state energies are lower than that of a metallic state, because they may reduce electron repulsion which has not been treated explicitly in the one-electron description. Therefore one-electron total electronic energies $\mathscr{E}$ often are basically inappropriate to predict the relative stability of the metallic and the insulating states of a partially filled energy band. Only the prediction of non-magnetic insulating states characterized by completely filled valence bands and broad HOCO-LUCO energy gaps seems to be unambiguous.

2.6 *Mulliken Population Analysis*

In a basis of $\dim V_{k,\Gamma_m}$ symmetry orbitals (14), the density matrix $\mathbf{P}(k, \Gamma_m)$ is defined by

$$\mathbf{P}(k, \Gamma_m) \equiv \mathbf{C}(k, \Gamma_m)\, \mathbf{n}(k, \Gamma_m)\, \mathbf{C}^\dagger(k, \Gamma_m)\,, \tag{35}$$

where $\mathbf{n}(k, \Gamma_m)$ is the diagonal matrix of the occupation numbers. There is no unique definition of the number of electrons to be associated with a given atom or atomic core in a one-dimensional crystal, but it is still sometimes useful to perform such population analyses [11]. Since K is the total number of all valence electrons per unit cell of a one-dimensional crystal, we get for a given set of N_k wavenumbers k (using (14) and (35))

$$\begin{aligned} N_k \cdot K &= \sum_k \sum_{\Gamma_m} \sum_{i=1}^{\dim V_{k,\Gamma_m}} n_i(k, \Gamma_m) \langle \Psi_i(k, \Gamma_m) \,|\, \Psi_i(k, \Gamma_m) \rangle \\ &= \sum_k \sum_{\Gamma_m} \sum_{\mu=1}^{\dim V_{k,\Gamma_m}} (\mathbf{P}(k, \Gamma_m)\, \mathbf{S}(k, \Gamma_m))_{\mu\mu} \\ &= \sum_k \sum_{\Gamma_m} \mathrm{tr}(\mathbf{Q}(k, \Gamma_m))\,, \end{aligned} \tag{36}$$

where we have introduced the abbreviating notation

$$\mathbf{Q}(k, \Gamma_m) \equiv \mathbf{P}(k, \Gamma_m)\, \mathbf{S}(k, \Gamma_m)\,. \tag{37}$$

The Mulliken population analysis interprets $Q_{\mu\mu}(k, \Gamma_m)$ as the number of electrons to be associated with the symmetry orbital $\Phi_\mu(k, \Gamma_m)$.

Because these symmetry-adapted Bloch sums are centered on equivalent atomic nuclei, the number of electrons to be associated with a given atom are obtained by taking the arithmetic mean over all symmetry orbitals centered on the corresponding atomic family. The net charge q_A associated with an atom A representing N_A *equivalent* atoms within one unit cell is then given by

$$q_\mathrm{A} = Z_\mathrm{A} - \frac{1}{N_k N_\mathrm{A}} \sum_k \sum_{\Gamma_m} \sum_{\mu \in \mathrm{A}} Q_{\mu\mu}(k, \Gamma_m)\,, \tag{38}$$

where Z_A is the charge of the atomic core of A; the indices of summation indicate that we only sum over the basis functions centered on equivalent nuclei of type A as well as over all irreducible representations Γ_m and all wavenumbers k of the line group symmetry under consideration.

It is a well-known feature of Mulliken population analysis that a slightly negative gross population occurs in cases where a sum of negative overlap populations predominates the positive Mulliken net population of the corresponding real basis orbital [21]. A similar artifact of complex Mulliken population analysis is, that imaginary parts of such gross populations sometimes do not vanish completely which is physically unreasonable.

2.7 *Valence Orbital Ionization Potentials*

As already mentioned, the VOIP of electrons in diverse atomic orbitals are taken to parametrize the diagonal elements of an extended-Hückel matrix $\mathbf{H}(k, \Gamma_m)$.

Unlike atoms in a homogeneous chemical environment of the same kind, heteropolarly bound atoms

are partially charged. Moreover, the sums Δ, Σ and Π of their d, s, and p valence orbital populations considerably differ from the configurations $d^{\Delta} s^{\Sigma} p^{\Pi}$ of the neutral atoms in uniform surroundings. Atomic charges q and valence orbital configurations $d^{\Delta} s^{\Sigma} p^{\Pi}$, however, exercise an unneglectable influence on the VOIP of a valence electron. According to the Mulliken population scheme, valence orbital populations Δ_A, Σ_A, and Π_A of an atom A representing N_A equivalent atoms within one unit cell can be calculated as follows:

$$\Delta_A = \frac{1}{N_k N_{d,A}} \sum_k \sum_{\Gamma_m} \sum_{\mu \in d,A} Q_{\mu\mu}(k, \Gamma_m), \quad (39)$$

$$\Sigma_A = \frac{1}{N_k N_{s,A}} \sum_k \sum_{\Gamma_m} \sum_{\mu \in s,A} Q_{\mu\mu}(k, \Gamma_m), \quad (40)$$

$$\Pi_A = \frac{1}{N_k N_{p,A}} \sum_k \sum_{\Gamma_m} \sum_{\mu \in p,A} Q_{\mu\mu}(k, \Gamma_m). \quad (41)$$

The sum of Δ_A, Σ_A, and Π_A is equal to the atomic population of a representative center within a whole family A of symmetrically equivalent atoms:

$$\Delta_A + \Sigma_A + \Pi_A = \frac{1}{N_k N_A} \sum_k \sum_{\Gamma_m} \sum_{\mu \in A} Q_{\mu\mu}(k, \Gamma_m). \quad (42)$$

For some first row transition metals (A $\in$ {Ti, V, Cr, Mn, Fe, Co, Ni}), Basch, Viste, and Gray [10] fitted quadratic polynomials in q_A

$$V_{i,A}^{\{j\}}(q_A) = A_{i,A}^{\{j\}}(q_A)^2 + B_{i,A}^{\{j\}}(q_A) + C_{i,A}^{\{j\}} \quad (43)$$

with the adjustable coefficients $A_{i,A}^{\{j\}}$, $B_{i,A}^{\{j\}}$ and $C_{i,A}^{\{j\}}$ on the empirically observed dependence of a VOIP $V_{i,A}^{\{j\}}$ (i $\in$ {s, p, d}) from the corresponding integer atomic and ionic charges q_A with respect to some selected electronic configurations {j} (j $\in$ {1, 2, 3}).

With such standard configurations listed in Table 1, the VOIP for fractional valence orbital configurations of these first row transition metals can be evaluated by means of the following formulas (Ballhausen and Gray [10]):

$$V_{d,A}(\Delta_A, \Sigma_A, \Pi_A) = (1 - \Sigma_A - \Pi_A)\, V_{d,A}^{\{1\}} + \Sigma_A\, V_{d,A}^{\{2\}} + \Pi_A\, V_{d,A}^{\{3\}}, \quad (44)$$

$$V_{s,A}(\Delta_A, \Sigma_A, \Pi_A) = (2 - \Sigma_A - \Pi_A)\, V_{s,A}^{\{1\}} + (\Sigma_A - 1)\, V_{s,A}^{\{2\}} + \Pi_A\, V_{s,A}^{\{3\}}, \quad (45)$$

$$V_{p,A}(\Delta_A, \Sigma_A, \Pi_A) = (2 - \Sigma_A - \Pi_A)\, V_{p,A}^{\{1\}} + (\Pi_A - 1)\, V_{p,A}^{\{2\}} + \Sigma_A\, V_{p,A}^{\{3\}}. \quad (46)$$

Table 1. Standard configurations for valence orbitals of Ti, V, Cr, Mn, Fe, Co, and Ni.

Valence orbital	Standard configuration		
	{1}	{2}	{3}
3 d	d^n	$d^{n-1} s$	$d^{n-1} p$
4 s	$d^{n-1} s$	$d^{n-2} s^2$	$d^{n-2} sp$
4 p	$d^{n-1} p$	$d^{n-2} p^2$	$d^{n-2} sp$

n: number of valence electrons of the transitional metal ($n = q + \Delta + \Sigma + \Pi$).

Table 2. Standard configurations for valence orbitals of second period elements.

Valence orbital	Standard configuration	
	{1}	{2}
2 s	$s^2 p^{n-2}$	sp^{n-1}
2 p	$s^2 p^{n-2}$	sp^{n-1}

n: number of valence electrons of the second period element ($n = q + \Sigma + \Pi$).

A similar set of standard configurations (cf. Table 2) and interpolation formulas can be set up for elements with only s and p valence electrons:

$$V_{s,A}(\Sigma_A, \Pi_A) = (\Sigma_A - 1)\, V_{s,A}^{\{1\}} + (2 - \Sigma_A)\, V_{s,A}^{\{2\}}, \quad (47)$$

$$V_{p,A}(\Sigma_A, \Pi_A) = (\Sigma_A - 1)\, V_{p,A}^{\{1\}} + (2 - \Sigma_A)\, V_{p,A}^{\{2\}}. \quad (48)$$

Methodical refinements for the parametrization of the diagonal elements of an extended-Hückel matrix $\mathbf{H}(k, \Gamma_m)$ can be introduced using iterative one-electron SCC (Self-Consistence of Charge) and SCCC (Self-Consistence of Charge and Configuration) procedures.

2.7.1 *Self-Consistence of Charge*

The flow chart in Fig. 1 explains the iterative algorithm of the SCC model.

One starts with guessed charges $q_A^{(0)}$ for the representatives of all N_F symmetrically *inequivalent* atomic families A, and evaluates the corresponding $V_{i,A}^{\{j\}}(q_A^{(0)})$ for all valence orbitals of *one* chosen configuration {j}.

Self-consistence of charge has been achieved whenever the atomic charges q_A of all N_F inequiv-

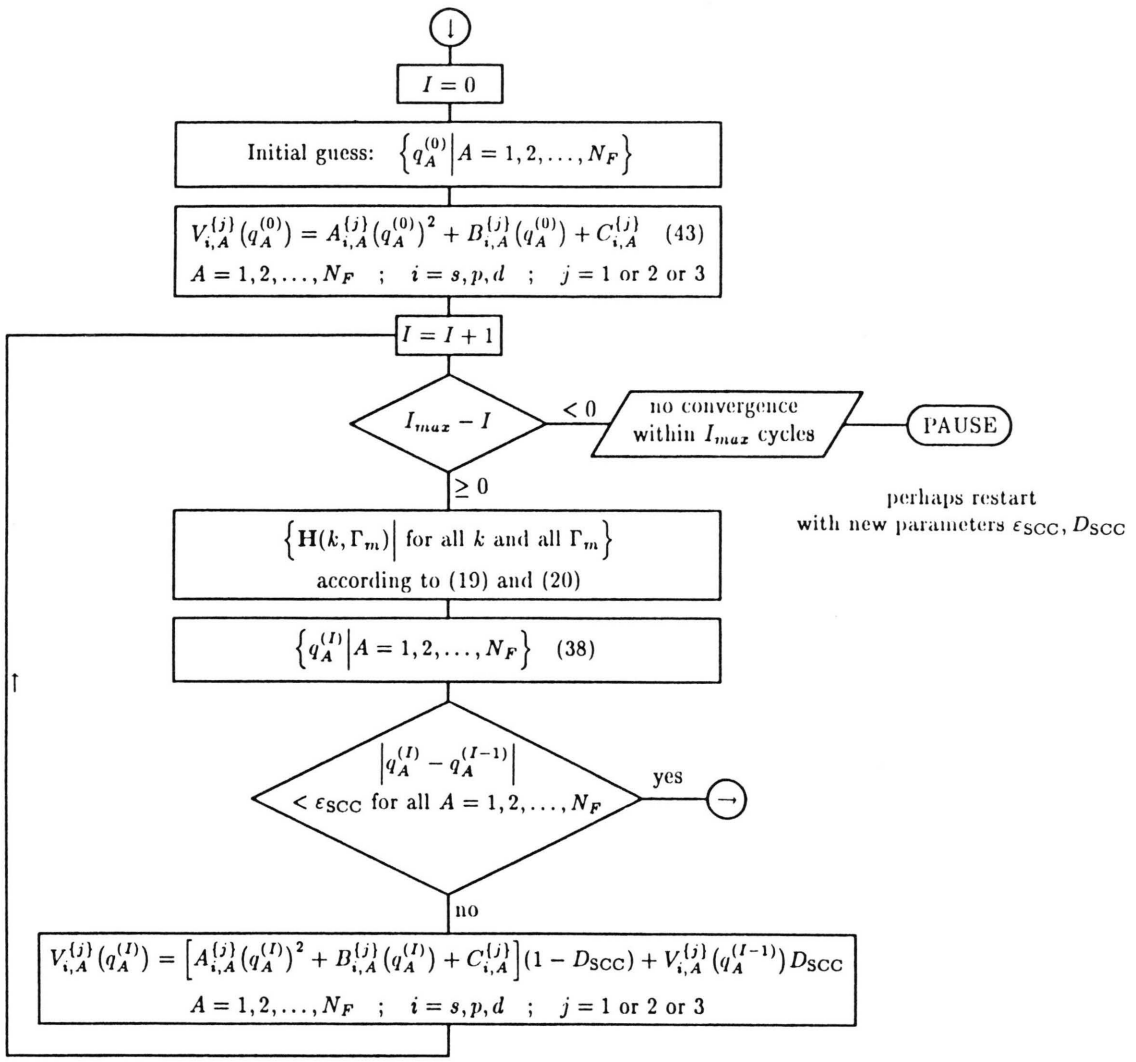

Fig. 1. Algorithm of the SCC procedure.

alent atoms do not change essentially within two subsequent iterative cycles I. The quality of the self-consistence procedure can be influenced by a suitable choice of the parameter ε_{SCC} which determines the break-off of the iteration. If convergence cannot be reached, the SCC procedure stops after having exceeded a previously set up maximum number I_{max} of steps.

If the energetical order of differently occupied crystal orbitals changes in the course of the iterative process, charge oscillations with a period of only a few cycles may occur. Particularly, if nearly degenerate crystal orbitals belong to energy bands of different symmetry labels Γ_m, a damping factor

$$0 \leqq D_{SCC} < 1 \tag{49}$$

has to be introduced in order to throttle charge oscillations and to promote the convergence.

2.7.2 *Self-Consistence of Charge and Configuration*

The SCCC procedure differs from the SCC iteration in guessing not only the charges $q_A^{(0)}$, but also the start configurations $d^{\Delta_A^{(0)}} s^{\Sigma_A^{(0)}} p^{\Pi_A^{(0)}}$ of all N_F

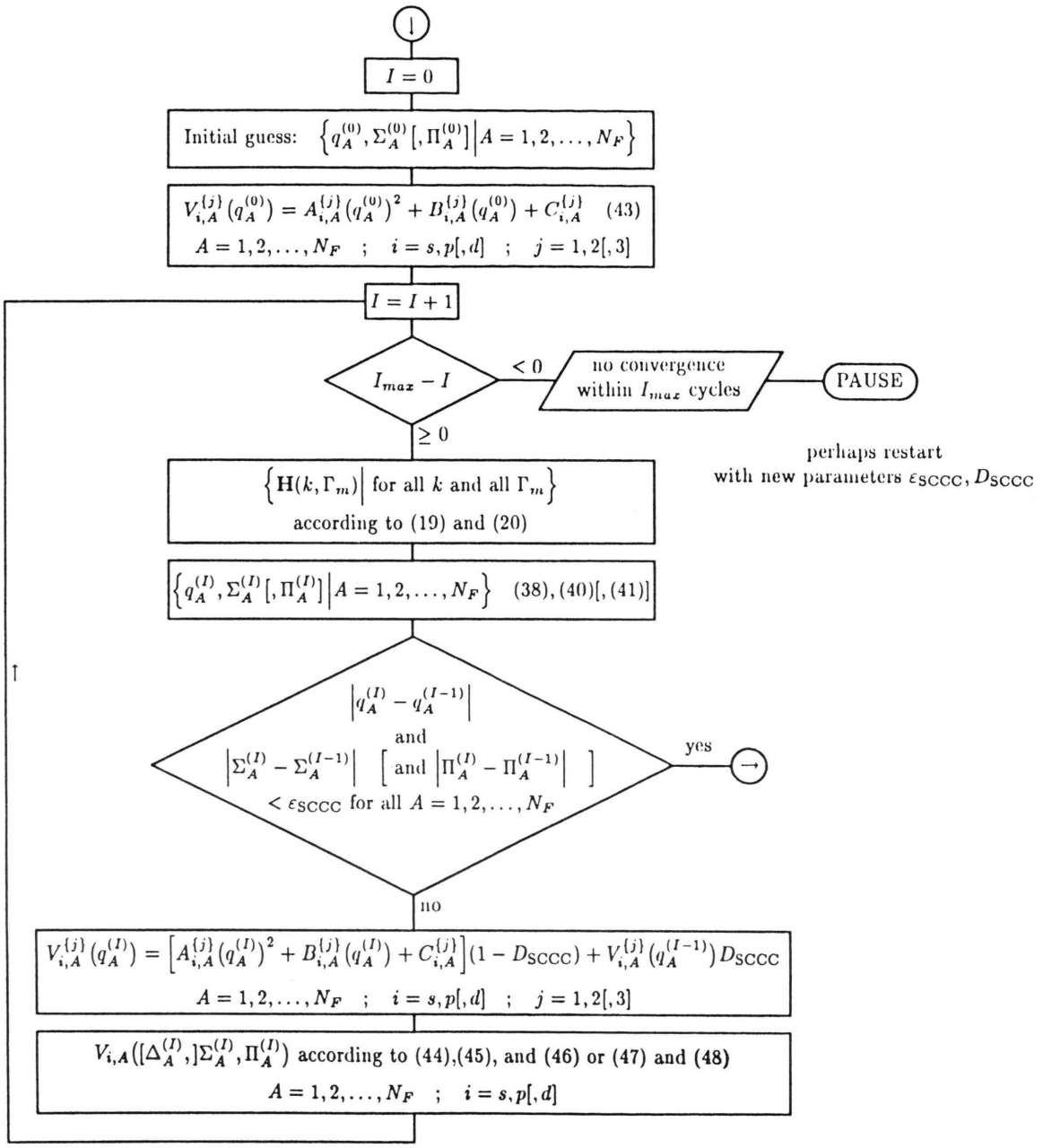

Fig. 2. Algorithm of the SCCC procedure.

symmetrically inequivalent atoms. The iteration is continued until the atomic charges q_A as well as their corresponding populations Δ_A, Σ_A, and Π_A do not differ essentially between two subsequent cycles. Like in the SCC model we introduce ε_{SCCC} and D_{SCCC} as convergence and damping parameters of the SCCC approach.

For the second row elements with a valence orbital configuration $s^{\Sigma} p^{\Pi}$, the evaluation of populations $\Pi_A^{(I)}$ and VOIP $V_{d,A}^{\{3\}}(q_A^{(I)})$ is actually not

needed (cf. Fig. 2, where these quantities have been put in brackets).

2.8 *Orbital Composition, Bond Order, Valence, and Free Valence*

In addition to atomic charges q and valence orbital populations Δ, Σ and Π, there are still some other quantities suitable to connect quantum chemical results and traditional chemical concepts.

$100 \cdot O^{(v)}_{i,A}(k, \Gamma_m)$, for instance, is a number which represents the percentage of the i-type symmetry orbitals ($i \in \{s, p, d\}$) of an atomic family A in a crystal orbital $\Psi_v(k, \Gamma_m)$ [22]:

$$O^{(v)}_{i,A}(k, \Gamma_m) = \sum_{\mu \in i,A} C^*_{\mu v}(k, \Gamma_m)\,(\mathbf{S}(k, \Gamma_m)\,\mathbf{C}(k, \Gamma_m))_{\mu v}. \tag{50}$$

As in Mulliken population analysis it may happen that some $O^{(v)}_{i,A}(k, \Gamma_m)$ show a small non-vanishing imaginary part.

For the calculation of on-site bond orders between the nearest neighbors of two atomic families such as valences and free valences of single centers, we used the recommended definitions of Mayer [23] to specify analogous expressions for one-dimensional crystals:

Bond order $B_{AA'}$ between next neighbors of two atomic families A and A':

$$B_{AA'} = \frac{1}{N_k N_A N_{A'}} \sum_k \sum_{\Gamma_m} \sum_{\mu \in A} \sum_{v \in A'} Q_{\mu v}(k, \Gamma_m)\, Q_{v\mu}(k, \Gamma_m). \tag{51}$$

Valence V_A of an atom belonging to the family A:

$$V_A = \frac{1}{N_k N_A} \sum_k \sum_{\Gamma_m} \left(2 \sum_{\mu \in A} Q_{\mu\mu}(k, \Gamma_m) - \sum_{\mu \in A} \sum_{v \in A} Q_{\mu v}(k, \Gamma_m)\, Q_{v\mu}(k, \Gamma_m)\right). \tag{52}$$

Free valence F_A of an atom belonging to the family A:

$$F_A = V_A - \sum_{A' \neq A} N_{A'} B_{AA'}. \tag{53}$$

For (closed-shell) systems without partially filled crystal orbitals, F_A is always equal to zero.

Bond orders, valences and free valences which have been computed according to the above definitions usually are not integers, but they do not deviate very much from the integer numbers of classical valence theory. Slightly negative values and small imaginary parts cannot be excluded, however.

2.9 *Density of States Histogram*

The ith segment $D(E_i)$ of a density of states histogram

$$\{D(E_i) \mid i = 1, \ldots, n_E\} \tag{54}$$

may be regarded as a measure for the number of allowed crystal orbital energies within a small energy interval ΔE of average energy E_i.

In this section we describe the construction of a density of states histogram for a non-degenerate energy band μ with symmetry label Γ_m whose energy values $E_{\Gamma_m,\mu}(k)$ are only known for the N_k considered wavenumbers $k_1 < k_2 < k_3 < \ldots < k_{N_k}$. If we divide the range $0 \leqq k \leqq \frac{\pi}{a}$ into n_k intervals of length Δk, and the energy scale spanned by all eigenvalues $E_\mu(k, \Gamma_m)$ into n_E intervals of length ΔE with average energies E_i ($i = 1, \ldots, n_E$), we get a grid of $n_k \cdot n_E$ rectangles with side lengths Δk and ΔE.

For each irreducible representation Γ_m and each energy band μ we define a function $I_{\Gamma_m,\mu}(E_i)$ as

$$I_{\Gamma_m,\mu}(E_i) = \sum_{j=1}^{n_k} \begin{cases} 1 & \text{if } \left(E_i - \frac{\Delta E}{2}\right) < E_{\Gamma_m,\mu}(k) \leqq \left(E_i + \frac{\Delta E}{2}\right) \text{ and } \frac{1}{n_k}(j-1)\frac{\pi}{a} < k \leqq \frac{1}{n_k} j \frac{\pi}{a} \\ 0 & \text{otherwise} \end{cases} \tag{55}$$

The sum $I(E_i)$ over all Γ_m and all μ of these functions

$$I(E_i) = \sum_{\Gamma_m} \sum_{\mu} I_{\Gamma_m,\mu}(E_i) \tag{56}$$

is equal to the number of grid rectangles which are intersected by the continuously interpolated curve $E_{\Gamma_m,\mu}(k)$.

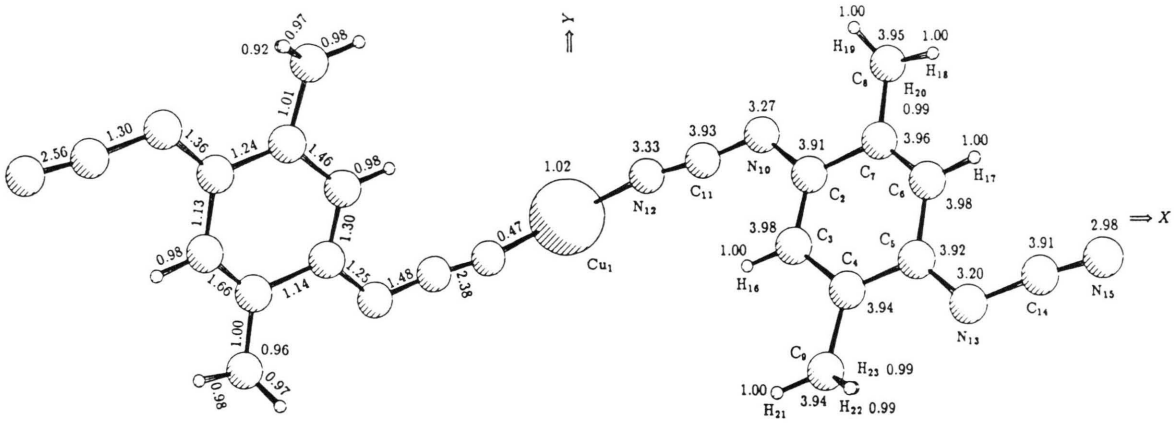

Fig. 3. Labelling, valences and on-site bond orders for all atomic families of $(2,5\text{-DM-DCNQI})_2Cu$.

Finally, the density of states $D(E_i)$ in an interval of average energy E_i is defined as

$$D(E_i) = I(E_i)/I_{\max}, \tag{57}$$

where $I_{\max}$ is the maximum of all integers $\{I(E_i) \mid i = 1, \ldots, n_E\}$.

The basic requirement for such a construction of a density of states histogram is, that the energy band structure, i .e. the continuous curves $E_{\Gamma_m,\mu}(k)$ are known for all band indices μ and all irreducible representations Γ_m. This complete energy band structure can be gained only approximately by means of an appropriate interpolation procedure.

We use a cubic spline function $E_{\Gamma_m,\mu}(k)$ [24] composed of $N_k - 1$ cubic polynomials

$$f_i(k) = A_i(k - k_i)^3 + B_i(k - k_i)^2 + C_i(k - k_i) + D_i, \quad i = 1, \ldots, N_k - 1 \tag{58}$$

defined in the ranges $[k_i, k_{i+1}]$, respectively. With the spline conditions:

$$\begin{aligned} f_i(k_i) &= f_{i-1}(k_i) = \mathrm{E}_\mu(k_i, \Gamma_m), \\ f_i'(k_i) &= f_{i-1}'(k_i), \quad i = 2, \ldots, N_k - 1 \\ f_i''(k_i) &= f_{i-1}''(k_i), \end{aligned} \tag{59}$$

and two additional boundary conditions:

$$f_1'(k_1) = 0 \quad \text{and} \quad f_{N_k-1}'(k_{N_k}) = 0 \tag{60}$$

we can get a system of N_k equations for the N_k unknown second derivatives $\{f_i''(k_i) \mid i = 1, \ldots, N_k\}$ from which the $4(N_k - 1)$ spline coefficients A_i, B_i, C_i, and D_i can be determined.

3. One-Dimensional Energy Band Structure of Bis(2,5-dimethyl-N,N′-dicyanoquinonediimine)-copper(I)

The first task of any one-dimensional energy band structure calculation is to choose an appropriate one-dimensional model geometry which can be assumed to represent the spatial and chemical structure of the real three-dimensional crystal. Figure 3 shows the one-dimensional unit cell (length $a = 3.881$ Å) of line group symmetry **L**2, because of its 2-fold rotation axis C_2 identical with the invariant line. Atomic coordinates (cf. Table 6) have been taken from crystallographic data, documented in reference [2]. Equivalent atomic families have been labelled as shown in Figure 3.

3.1 Parametrization

The band structure calculation has been performed according to the following list of standard choices:

1. The range $0 \leqq k \leqq \dfrac{\pi}{a}$ of the first Brillouin zone has been subdivided into five equidistant intervals; the $N_k = 6$ values of the wavenumber k therefore are 0.0, 0.2, 0.4, 0.6, 0.8 and 1.0 in units of $\left(\dfrac{\pi}{a}\right)$.
2. Starting with the VOIP recommended by Ballhausen and Gray [10] (cf. Table 3), valence orbital ionization potentials generally have been

evaluated by means of the iterative SCC and SCCC procedures, namely:
- VOIP of the elements H and Cu according to SCC,
- VOIP of the elements C and N according to SCCC.

We used the standard interpolation parameter sets of Basch, Viste, and Gray [10] for H, C, and N. SCC-parameters for Cu have been taken from reference [25] (cf. Table 5).

3. Convergence and damping parameters have been chosen in such a way that no charge oscillations could be observed:

$$\varepsilon_{\mathrm{SCC}} = \varepsilon_{\mathrm{SCCC}} = 0.05\,,$$
$$D_{\mathrm{SCC}} = D_{\mathrm{SCCC}} = 0.95\,.$$

In this way, convergence could be achieved within only a few iterative cycles. Unlike non-iterative extended-Hückel charge distributions, SCC and SCCC charges are in good agreement with chemical intuition.

4. Extended-Hückel matrices $\mathbf{H}(k, \Gamma_m)$ have been calculated according to (19) and (20) with the scaling factor F' defined in (21) and (22). Using this modified Wolfsberg-Helmholz formula, negative orbital populations can be avoided [7]. As usual, F has been set equal to 1.75 [26].
5. For the orbital exponents ζ we took the approved parameter sets of Whangbo, Hoffmann, and co-workers [27] (cf. Table 3):
   - s and p exponents have been taken from Slater [4],
   - linear combinations of two transition metal 3d Slater type orbitals have been used according to Richardson, Nieuwpoort, Powell, and Edgell [5] (cf. Table 4).
6. We set δ which controls the break-off of Bloch summation (6) equal to 10^{-12}.
7. Nearly degenerate crystal orbitals with an energy difference less than 10^{-6} eV have been occupied according to Hund's rule in the course of the iterative procedure.
8. We took

$$n_E = 1000 \quad \text{and} \quad n_k = 30000$$

to construct an appropriately resolved density of states grid (cf. (54) and (55)).

Table 3. Valence orbitals, exponents, and initial VOIP.

Atom	Valence orbital	ζ	VOIP ($10^3\,\mathrm{cm}^{-1}$)
H	1 s	1.0000	110
C	2 s	1.6250	157
C	2 p	1.6250	86
N	2 s	1.9500	206
N	2 p	1.9500	106
Cu	3 d		86
Cu	4 s	1.0000	62
Cu	4 p	1.0000	32

Table 4. Double-ζ exponents and coefficients.

Atom	Valence orbital	ζ_1	c_1	ζ_2	c_2
Cu	3 d	5.95	0.5933	2.30	0.5744

3.2 *Computational Results*

With the chosen set of valence orbitals (cf. Table 3), (2,5-DM-DCNQI)$_2$Cu contains 147 valence electrons. The SCC/SCCC procedure converged after 7 iteration cycles. Overlap integrals of 15 unit cells have been added according to (4) until condition (6) could be fulfilled ($N_{\max} = 7$).

Using symmetry adapted linear combinations of Bloch sums, the eigenvalue problem (2) splitted into two equations (11) with the matrix dimensions $\dim V_{k,A_0} = 69$ and $\dim V_{k,A_1} = 68$, respectively.

Table 5. SCC and SCCC interpolation parameters (in $10^3\,\mathrm{cm}^{-1}$).

Atom	Valence orbital	$A\{1\}$	$B\{1\}$	$C\{1\}$	$A\{2\}$	$B\{2\}$	$C\{2\}$
H	1 s	109.84	219.20	109.70			
C	2 s	27.95	141.60	156.60	28.00	141.20	171.00
C	2 p	27.95	118.20	85.80	28.03	111.95	86.90
N	2 s	28.16	162.20	206.20	28.05	163.30	226.00
N	2 p	28.16	133.20	106.40	30.01	114.00	129.40
Cu	3 d	32.91	45.41	85.98			
Cu	4 s	7.60	71.30	62.27			
Cu	4 p	8.47	53.55	32.10			

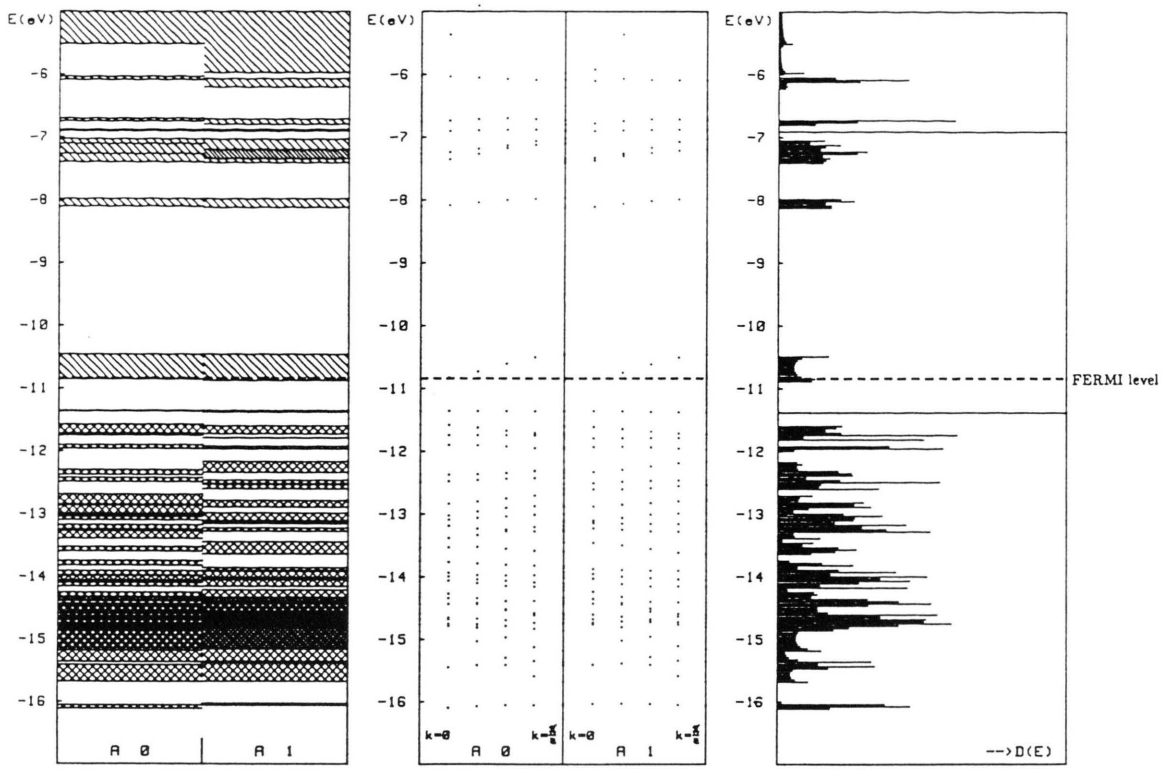

Fig. 4. One-dimensional energy band structure and density of states histogram.

Table 6. Cartesian coordinates X, Y and Z, valence orbital ionization potentials V, configurations $d^{\Delta} s^{\Sigma} p^{\Pi}$ and charges q for all representative atoms of $(2,5\text{-DM-DCNQI})_2Cu$.

Atomic family	X (Å)	Y (Å)	Z (Å)	V(d) (10^3 cm^{-1})	V(s) (10^3 cm^{-1})	V(p) (10^3 cm^{-1})	Δ	Σ	Π	q (a.u.)
Cu_1	0.000	0.000	−3.881	112.51752	83.05280	49.07945	9.92	0.32	0.29	0.47
C_2	4.526	0.757	−1.256	0.00000	169.91946	94.03606	0.00	1.15	2.75	0.10
C_3	4.189	−0.558	−0.925	0.00000	159.51662	85.55800	0.00	1.09	2.88	0.04
C_4	5.077	−1.349	−0.154	0.00000	164.61484	89.79810	0.00	1.16	2.77	0.07
C_5	6.285	−0.800	0.302	0.00000	170.18992	94.21698	0.00	1.14	2.76	0.10
C_6	6.558	0.607	−0.056	0.00000	159.41989	85.44521	0.00	1.07	2.90	0.03
C_7	5.801	1.351	−0.782	0.00000	163.07280	88.51740	0.00	1.15	2.81	0.05
C_8	6.041	2.795	−1.176	0.00000	152.87153	80.13189	0.00	0.98	3.12	−0.10
C_9	4.636	−2.777	0.121	0.00000	153.47573	80.60048	0.00	0.98	3.10	−0.09
N_{10}	3.718	1.539	−2.005	0.00000	192.16803	97.65166	0.00	1.34	3.90	−0.24
C_{11}	2.607	1.074	−2.468	0.00000	174.95593	98.19057	0.00	1.14	2.80	0.06
N_{12}	1.558	0.789	−2.934	0.00000	188.55541	94.83951	0.00	1.42	3.83	−0.25
N_{13}	7.064	−1.552	1.064	0.00000	191.16342	96.92589	0.00	1.35	3.89	−0.25
C_{14}	8.226	−1.048	1.542	0.00000	174.57725	97.88861	0.00	1.14	2.83	0.03
N_{15}	9.210	−0.739	2.012	0.00000	186.70224	93.44695	0.00	1.46	3.83	−0.30
H_{16}	3.346	−0.925	−1.203	0.00000	114.00869	0.00000	0.00	0.94	0.00	0.06
H_{17}	7.360	0.999	0.297	0.00000	114.38491	0.00000	0.00	0.93	0.00	0.07
H_{18}	6.778	2.929	−0.576	0.00000	115.76542	0.00000	0.00	0.93	0.00	0.07
H_{19}	5.360	3.445	−0.995	0.00000	114.81561	0.00000	0.00	0.95	0.00	0.05
H_{20}	6.346	2.890	−2.081	0.00000	115.43294	0.00000	0.00	0.94	0.00	0.06
H_{21}	3.763	−3.158	−0.012	0.00000	114.63848	0.00000	0.00	0.95	0.00	0.05
H_{22}	4.945	−2.993	1.004	0.00000	115.30735	0.00000	0.00	0.94	0.00	0.06
H_{23}	5.244	−3.138	−0.528	0.00000	116.93741	0.00000	0.00	0.92	0.00	0.08

In Table 6, valence orbital ionization potentials V, populations Δ, Σ and Π such as atomic charges q of the 7th iteration step have been listed. It shows that copper 4s and 4p orbitals are only slightly populated. As expected, atomic charges of the electronegative nitrogen atoms are always negative; copper atoms are positively charged (0.47 a.u.).

Calculated valences and bond orders have been inserted into Figure 3. The discrepancy between these valences and the integer values of chemical valence theory is very small. Bond orders in the range between 1 and 2 emphasize the aromatic character of the quinoid ring systems. Cu atoms are strongest bound to next neighbor nitrogens, of course, with a bond order of 0.47.

Figure 4 shows the energy band structure and the density of states histogram in the energy range between -17 eV and -5 eV. Each point of the central diagram represents the energy $E_\mu(k, \Gamma_m)$ of the crystal orbital $\Phi_\mu(k, \Gamma_m)$. Allowed and forbidden zones, bandwidths and band gaps can be recognized best by inspecting the left block chart. Near the Fermi level (-10.84 eV) there are only two energy bands belonging to the irreducible representations A_0 and A_1, respectively, which nearly overlap each other completely.

If we focus on the two antipodal possibilities of band occupancy, namely the metallic versus the magnetic insulating (MOTT) state, a complete occupation of both energy bands with electrons of identical spin is not achievable because only 1/3 of the 37 A_1 band is occupied (wavenumbers $k = 0$ and $k = 0.2\,\frac{\pi}{a}$) and only 1/6 of the 38 A_0 band (wavenumber $k = 0$). Although the combined width (0.42 eV) of both energy bands is rather small, we therefore predict a metallic state to be most stable, resulting from the incomplete occupancy of both 38 A_0 and 37 A_1 energy bands. This is the most important result; it is in good agreement with the experiment [2]. For the non-magnetic metallic characteristic the total electronic ground state energy $\mathscr{E}$ (cf. (34)) yields -2496.35 eV.

Table 7 shows the percental composition (50) of the crystal orbitals $\Psi_{37}(k, A_1)$ and $\Psi_{38}(k, A_0)$; in both energy bands there is no significant participation of Cu electrons at all. We conclude that the copper atoms do not play any role in the mechanism of electronic conductivity, as already presumed in [2].

4. Conclusion

Though we cannot expect that relative stabilities of metallic and insulating states are unambiguously determinable within one-electron theories, one-dimensional band structure calculations of extended-Hückel type may be useful to rationalize the observed electronic properties of quasi one-dimensional crystals, as could be demonstrated for the highly conducting compound (2,5-DM-DCNQI)$_2$Cu.

In addition to considerable computational savings which can be achieved by using symmetry adapted linear combinations of Bloch sums as basis func-

Table 7. Composition of the two incompletely occupied energy bands 38 A_0 and 37 A_1.

38 A_0	
$k = 0.0$:	21% $N_{13}p$, 15% $N_{10}p$, 12% $N_{12}p$, 12% $N_{15}p$, 9% C_2p, 9% C_5p, 8% C_4p, 4% C_7p, 2% C_3p, 2% C_6p
$k = 0.2$:	21% $N_{13}p$, 15% $N_{10}p$, 12% $N_{12}p$, 12% $N_{15}p$, 9% C_2p, 9% C_5p, 8% C_4p, 4% C_7p, 3% C_3p, 3% C_6p
$k = 0.4$:	21% $N_{13}p$, 13% $N_{10}p$, 11% $N_{12}p$, 10% C_2p, 10% C_5p, 10% $N_{15}p$, 9% C_4p, 4% C_7p, 3% C_3p, 3% C_6p
$k = 0.6$:	21% $N_{13}p$, 13% $N_{10}p$, 12% C_2p, 11% C_5p, 9% C_4p, 9% $N_{12}p$, 9% $N_{15}p$, 5% C_3p, 4% C_7p, 3% C_6p
$k = 0.8$:	21% $N_{13}p$, 13% C_2p, 13% $N_{10}p$, 12% C_5p, 10% C_4p, 9% $N_{15}p$, 8% $N_{12}p$, 5% C_3p, 4% C_6p, 4% C_7p
$k = 1.0$:	21% $N_{13}p$, 13% C_2p, 13% $N_{10}p$, 12% C_5p, 10% C_4p, 8% $N_{12}p$, 8% $N_{15}p$, 5% C_3p, 4% C_6p, 4% C_7p
37 A_1	
$k = 0.0$:	23% $N_{13}p$, 13% $N_{10}p$, 12% $N_{12}p$, 12% $N_{15}p$, 10% C_2p, 10% C_4p, 9% C_5p, 4% C_7p, 2% C_6p, 2% C_9p
$k = 0.2$:	22% $N_{13}p$, 13% $N_{10}p$, 12% $N_{15}p$, 11% $N_{12}p$, 10% C_2p, 10% C_4p, 9% C_5p, 4% C_7p, 3% C_6p, 1% C_3p
$k = 0.4$:	22% $N_{13}p$, 13% $N_{10}p$, 11% C_2p, 11% $N_{15}p$, 10% C_4p, 10% C_5p, 10% $N_{12}p$, 4% C_7p, 3% C_3p, 3% C_6p
$k = 0.6$:	21% $N_{13}p$, 13% $N_{10}p$, 12% C_2p, 11% C_5p, 9% C_4p, 9% $N_{12}p$, 9% $N_{15}p$, 5% C_3p, 4% C_7p, 3% C_6p
$k = 0.8$:	21% $N_{13}p$, 14% $N_{10}p$, 13% C_2p, 12% C_5p, 9% C_4p, 9% $N_{15}p$, 8% $N_{12}p$, 5% C_3p, 4% C_6p, 4% C_7p
$k = 1.0$:	21% $N_{13}p$, 14% $N_{10}p$, 13% C_2p, 12% C_5p, 10% C_4p, 8% $N_{15}p$, 7% $N_{12}p$, 5% C_3p, 4% C_6p, 4% C_7p

tions, the main advantage of our treatment is that band indexing difficulties and any consequent misinterpretations of the electronic band structure are systematically excluded. Moreover, it has the nice feature that the evaluation of extended-Hückel matrix elements as well as the computation of atomic charges, populations, valences, and bond orders can be performed within this symmetry basis throughout, so that no backtransformations into the original atomic orbital basis are ever needed.

Acknowledgement

This work has been supported by the *Stiftung Volkswagenwerk* which is gratefully acknowledged.

[1] M. C. Böhm, Theor. Chim. Acta (Berlin) **62,** 351 (1983).
[2] A. Aumüller, P. Erk, G. Klebe, S. Hünig, J. U. von Schütz, and H.-P. Werner, Angew. Chem. **98,** 759 (1986); Angew. Chem. Int. Ed. Engl. **25,** 740 (1986).
[3] W. Koch and F. F. Seelig, Int. J. Quantum Chem. **32** (1987), in press.
[4] J. C. Slater, Phys. Rev. **36,** 57 (1930). – E. Clementi and D. L. Raimondi, J. Chem. Phys. **38,** 2686 (1963). G. Burns, J. Chem. Phys. **41,** 1521 (1964).
[5] J. W. Richardson, W. C. Nieuwpoort, R. R. Powell, and W. F. Edgell, J. Chem. Phys. **36,** 1057 (1962).
[6] D. M. Silver and K. Ruedenberg, J. Chem. Phys. **49,** 4301 (1968).
[7] M. Wolfsberg and L. Helmholz, J. Chem. Phys. **20,** 837 (1952). – C. J. Ballhausen and H. B. Gray, Inorg. Chem. **1,** 111 (1962). – L. C. Cusachs, J. Chem. Phys. **43,** S 157 (1965). – W. A. Yeranos, J. Chem. Phys. **44,** 2207 (1966). – J. H. Ammeter, H.-B. Bürgi, J. C. Thibeault, and R. Hoffmann, J. Amer. Chem. Soc. **100,** 3686 (1978).
[8] In a symmetry-adapted linear combination $\Phi_\mu(k, \Gamma_m)$, only equivalent Bloch sums $\Phi_\mu(k)$ with identical valence orbital ionization potentials V_μ are combined.
[9] F. F. Seelig, Z. Naturforsch. **37a,** 1158 (1982). – W. Koch, Extended-Hückel-Berechnung der Energiebandstruktur von Übergangsmetallverbindungen mit eindimensionaler Kristallgeometrie. Thesis, Universität Tübingen 1986.
[10] J. Hinze and H. H. Jaffé, J. Amer. Chem. Soc. **84,** 540 (1962). – J. Hinze and H. H. Jaffé, J. Phys. Chem. **67,** 1501 (1963). – C. J. Ballhausen and H. B. Gray, Molecular Orbital Theory: An Introductory Lecture Note and Reprint Volume. W. A. Benjamin Inc., New York 1964, pp. 92–132. – H. Basch, A. Viste, and H. B. Gray, Theor. Chim. Acta (Berlin) **3,** 458 (1965). – L. C. Cusachs and J. H. Corrington, Atomic Orbitals for Semiempirical Molecular Orbital Calculations, in: Sigma Molecular Orbital Theory (O. Sinanoğlu and K. B. Wiberg, eds.). Yale University Press, New Haven 1970, pp. 256–272.
[11] A. Szabo and N. S. Ostlund, Modern Quantum Chemistry: Introduction to Advanced Electronic Structure Theory. Macmillan Publishing Co., Inc. New York, Collier Macmillan Publishers, London 1982.
[12] There exist numerous efficient algorithms for the diagonalization of Hermitian matrices. FORTRAN eigenvalue routines which base upon such algorithms can be taken from the program package EISPACK [13], for instance.
[13] B. T. Smith, J. M. Boyle, J. J. Dongarra, B. S. Garbow, Y. Ikebe, V. C. Klema, and C. B. Moler, Matrix Eigensystem Routines – EISPACK Guide, 2nd edition. Springer-Verlag, Berlin 1976.
[14] Since $\mathbf{S}(k, \Gamma_m)$ is positive definite, i.e. its eigenvalues are all positive, there is in principle no difficulty of taking square roots.
[15] I. Božović and J. Delhalle, Phys. Rev. **B 29,** 4733 (1984).
[16] J.-M. André, Adv. Quantum Chem. **12,** 65 (1980).
[17] As a consequence, there is no need for an indexing procedure of an energy band $E_\mu(k)$ without symmetry label Γ_m by means of the first derivative with respect to k [18].
[18] J.-M. André, J. Delhalle, G. Kapsomenos, and G. Leroy, Chem. Phys. Lett. **14,** 485 (1972). – J. Delhalle, D. Thelen, and J.-M. André, Computers Chem. **3,** 1 (1979).
[19] In addition to the non-magnetic insulating states arising from completely occupied valence bands, some other insulating states caused by partially filled energy bands may be distinguishable [20], namely: *magnetic insulating (MOTT) states, spin density wave states, charge density wave states, bond density wave states.*
[20] M.-H. Whangbo, Acc. Chem. Res. **16,** 95 (1983).
[21] J. P. Lowe, Quantum Chemistry, Academic Press, Inc., New York 1978.
[22] F. F. Seelig, Z. Naturforsch. **34a,** 986 (1979).
[23] I. Mayer, Int. J. Quantum Chem. **26,** 151 (1984).
[24] H. Späth, Spline-Algorithmen zur Konstruktion glatter Kurven und Flächen. R. Oldenbourg Verlag, München 1973.
[25] P. J. Hay, J. C. Thibeault, and R. Hoffmann, J. Amer. Chem. Soc. **97,** 4884 (1975).
[26] R. Hoffmann, J. Chem. Phys. **39,** 1397 (1963).
[27] There are numerous contributions which are closely related to our treatment, for instance [28].
[28] M.-H. Whangbo and R. Hoffmann, J. Amer. Soc. **100,** 6093 (1978). – M.-H. Whangbo, R. Hoffmann, and R. B. Woodward, Proc. Roy. Soc. London **A 366,** 23 (1979). – M.-H. Whangbo, M. J. Foshee, and R. Hoffmann, Inorg. Chem. **19,** 1723 (1980). – M.-H. Whangbo and K. R. Stewart, Isr. J. Chem. **23,** 133 (1983).